DOI: 10.1002/ejic.200800128

Mo-Catalyzed Cross-Metathesis Reaction of Propynylferrocene

Tomáš Bobula,[a] Jason Hudlický,[a][‡] Petr Novák,[a] Róbert Gyepes,[b] Ivana Císařová,[b] Petr Štěpnička,*[b] and Martin Kotora*[a,c]

Keywords: Alkynes / Metallocenes / Metathesis / Electrochemistry / X-ray diffraction

Catalysts formed in situ from [$Mo(CO)_6$] and halophenols in dichloromethane efficiently promote cross metathesis reactions of (prop-1-yn-1-yl)ferrocene with various functionalized alkynes to give the corresponding alkynylferrocenes with good selectivity and yields. Optimization of the reaction conditions by changing the phenol component has been carried out, revealing a critical influence of the phenol structure on the reaction yield. The structures of selected compounds were determined by single-crystal X-ray diffraction, and the results (particularly the crystal packing) were correlated with DFT calculations. In addition, the series of alkynes 4-$XC_6H_4C{\equiv}CFc$ (Fc = ferrocenyl) differing by the substituent X was studied by electrochemical methods, manifesting a good correlation between the redox potential of the ferrocene/ferrocenium couple and the Hammett σ_p constants of the remote substituents X.

Introduction

In the last ten years, the scientific community has witnessed an enormous surge in the application of alkene metathesis toward many different areas of chemistry, including the synthesis of natural compounds and related substances, polymer chemistry, as well as organometallic synthesis. This development apparently reflects the ready availability of the metathesis catalysts, versatility of the reaction, and its tolerance to a wide range of functional groups.[1] By contrast, the analogous reaction involving alkynes (i.e., alkyne metathesis) has been developed much less, mostly because its application faces several problems, such as catalyst performance, unfavorable reaction conditions, limited compatibility with functional groups, etc. Nonetheless, as these obstacles are slowly but steadily eliminated, alkyne metathesis gains importance as a useful synthetic method. Thus, alkyne metathesis[2] has become an indispensable tool in natural product synthesis,[3] polymer and macromolecular chemistry,[4] and in organometallic chemistry.[5]

The catalytic systems used in alkyne metathesis can be classified into two groups: (i) structurally undefined catalysts formed "in situ" from of Mo[6] or W[7] carbonyls and phenols, and (ii) catalysts based on defined molybdenum[8] and tungsten[9] carbyne or molybdenum amide complexes.[10] Although the former catalytic systems are generally less reactive, they attract attention because of their simplicity. On the other hand, the unknown nature of the catalytically active species makes their use rather unpredictable, which, in turn, initiated attempts at refinement of the reaction conditions. It has been found that the reactivity of the metal carbonyl/phenol system can be improved by substituting resorcinol, used in the original Mortreux system,[6] by phenols bearing electron-withdrawing groups. Among them, the best results were achieved with halophenols such as 4-chlorophenol,[11,12] 4-(trifluoromethyl)phenol,[12] and 2-fluorophenol.[13] Other additives such as silanes[14] or ethers[15] were studied as well.

Although it has been clearly demonstrated that the scope of alkyne metathesis is very wide, its use in the synthesis of alkynes bearing organometallic fragments, namely metallocenyl groups, remains rather unexplored. So far, only three papers dealing with the homometathesis of metallocene alkynes have been published. The first two deal with the synthesis of bis(ruthenocenyl)ethynes,[16] while the last one reports the preparation of diferrocenylethyne.[17] In view of the foregoing discussion, it is rather surprising that alkyne cross-metathesis has not yet been studied with metallocenylalkynes, because it could potentially open a practical route to new metallocene derivatives, complementary to cross-coupling reactions.

[a] Department of Organic and Nuclear Chemistry and Centre for New Antivirals and Antineoplastics, Faculty of Science, Charles University,
Hlavova 8, 128 43 Praha 2, Czech Republic
Fax: +420-221-951-326
E-mail: kotora@natur.cuni.cz
[b] Department of Inorganic Chemistry, Faculty of Science, Charles University,
Hlavova 8, 128 43 Praha 2, Czech Republic
E-mail: stepnic@natur.cuni.cz
[c] Institute of Organic Chemistry and Biochemistry, v.v.i., Academy of Sciences of the Czech Republic,
Flemingovo nám. 2, 166 10 Praha 6, Czech Republic
[‡] Summer research participant. Current address: Ridley College, P. O. Box 3013, 2 Ridley Rd., St. Catharines ON L2R 7C3, Canada
Supporting information for this article is available on the WWW under http://www.eurjic.org or from the author.

Results and Discussion

Metathesis Reactions

Since it was shown that the $[Mo(CO)_6]$/2-fluorophenol system belongs to the most active "instant" catalysts,[13] we decided to use it as a standard catalyst for the cross-alkyne metathesis reaction of (prop-1-yn-1-yl)ferrocene (**1**). As the second alkyne component, we chose a range of arylalkynes bearing electron-donating and -withdrawing groups as well as some alkyl-substituted derivatives. The metathesis of **1** with various alkynes **2** was carried out in the presence $[Mo(CO)_6]$ (20 mol-%) and 2-fluorophenol (100 mol-%) in toluene at 120–125 °C (Scheme 1) under argon in a closed vial until complete consumption of the starting material was achieved (usually 1–3 h). Despite the rather harsh reaction conditions, the metathesis reaction proceeded well in all cases, affording the expected alkynylferrocenes **3** (Table 1) in good yields along with minor amounts of diferrocenylethyne (**4**) and disubstituted ethynes as the self-metathesis products (isolated in yields of 5–20%).

The reaction with electron-rich arylalkynes **2a** and **2b** furnished the corresponding products **3a** and **3b** in good isolated yields of 62 and 42%, respectively. Likewise, the metathesis with propynylbenzene (**2c**) and 4-(prop-1-yn-1-yl)-1,1′-biphenyl (**2d**) proceeded satisfactorily, giving alkynylferrocenes **3c** and **3d** in 63 and 59% yield, respectively. Alkyne **2e** bearing a COOMe group afforded **3e** in 54% yield, while somewhat lower yields (32 and 33%) were attained with ferrocenylalkynes **3f** and **3g** bearing stronger electron-withdrawing groups (CF_3, CN).

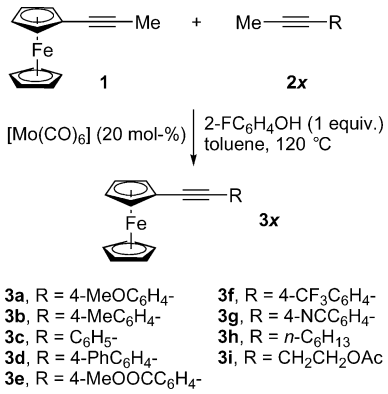

Scheme 1. Metathesis of 1-ferrocenylprop-1-yne (**1**) with alkynes **2** to give ferrocenylalkynes **3**.

Table 1. Metathesis of ferrocenylpropyne **1** with alkynes **2**.

Entry	Alkyne **2**	Alkynylferrocene **3**		Yield [%][a]
1	**2a**	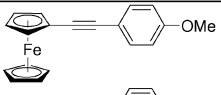	**3a**	62
2	**2b**	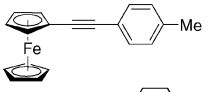	**3b**	42
3	**2c**	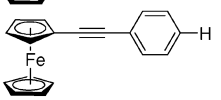	**3c**	63
4	**2d**	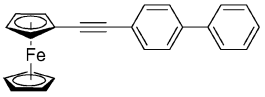	**3d**	59
5	**2e**	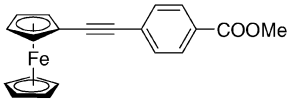	**3e**	54
6	**2f**	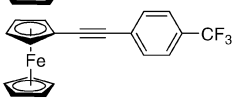	**3f**	32
7	**2g**	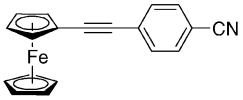	**3g**	33
8	**2h**	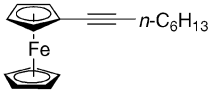	**3h**	64
9	**2i**	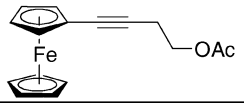	**3i**	27

[a] Isolated yields.

Table 2. Influence of various phenols on the reaction of **1** with alkynes **2e**.

Entry	Phenol	pK_A[a]	pK_A[b]	**3e**, Yield [%][c]
1	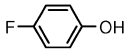	9.9[e]	9.92	63
2	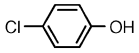	9.35[d]	9.74	49
3	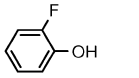	8.48[f]	8.71	54
4	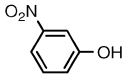	8.32[e]	8.33	0
5	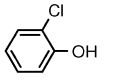	8.32[f]	8.50	62
6	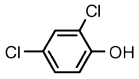	7.85[d]	8.04	48
7	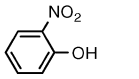	7.23[d]	7.14	0
8	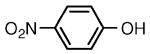	7.15[d]	7.22	0
9	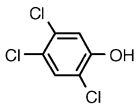	6.88[f]	n.a.	60
10	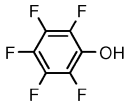	5.33[f]	5.50	80
11	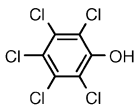	4.79[g]	n.a.	45

[a] For aqueous solutions. [b] Calculated values (ref.[13]), n.a.: not available. [c] Isolated yields. [d] Ref.[18a] [e] Ref.[18b] [f] Ref.[18c] [g] Ref.[18d]

The reaction with 2-octyne (**2h**) proceeded smoothly, giving rise to **3h** in 64% yield. By contrast, the metathesis with acetoxyalkyne **2i** gave the corresponding product **3i** in a rather low yield of 27%. Similar reactions with 2-(prop-1-yn-1-yl)pyridine and 2-(prop-1-yn-1-yl)thiophene were also checked, but the reaction did not take place. It is likely that the high Lewis acidity of the heteroatoms either did not allow the formation of the catalytically active species or led to its deactivation (e.g., by complexation of the Mo species).

Recently, we[17] and Grela et al.[13] showed that a combination of $[Mo(CO)_6]$ with other halogenated phenols could promote the formation of the catalytically active species. Additionally, it was suggested[13] that only phenols within a certain acidity (pK_a) range promote the formation of the catalytically active species. To verify whether this assumption is applicable also in this instance, we determined the catalytic activity of species resulting from a combination of $[Mo(CO)_6]$ and various phenols, using metathesis between **1** and **2e** as the model reaction (Table 2).

It is worth mentioning that the reaction proceeded to give the expected product **3e** in good yields in all cases when halogenated phenols were used (Table 2, Entries 1–3,5,6,9–11). Surprisingly, 4-fluorophenol (Entry 1), 2-chlorophenol (Entry 5), 2,4,5-trichlorophenol (Entry 9), and pentafluorophenol (Entry 10) furnished better yields of **3e** (63, 62, 60, and 80%) than that of the standard procedure[13] (Entry 3). Since the metathesis reaction took place even in the presence of more acidic phenols (Entries 9–11), it follows that the assumption concerning the influence of phenol acidity[13] does not apply in this case. Catalytic systems based on 2- and 4-nitrophenol (Entries 7 and 8) did not promote the reaction, which is in agreement with the previous reports.[13] Neither did the metathesis proceed with 3-nitrophenol (Entry 4).

In view of these results, we conclude that the ability of the $[Mo(CO)_6]$/phenol system to promote the metathesis reaction is compromised only partly with the acidity of the phenol component. An alternative explanation of the different reactivities could be sought in other properties of the 2- and 4-nitrophenols. For instance, it is known that 2- and 4-nitrophenols can exist in tautomeric forms[19] and may thus form a catalytically inactive species upon the reaction with $[Mo(CO)_6]$. This, however, does not account for the inability of the 3-nitrophenol-based catalyst to promote the reaction.

Crystallography

To study the influence of the benzene-ring substituents on the solid-state structure, we conducted single-crystal X-ray diffraction analysis for all compounds that yielded crystals of suitable quality. Although the structure of **3g** has already been reported,[20] we repeated its structural analysis to create a coherent data set with a minimal systematic bias due to dissimilar experimental conditions (e.g., temperature). The molecular structures of **3b**, **3e**, **3f**, and **3g** are shown in Figure 1, and geometric data are given in Table 3.

The molecular geometries of **3b**, **3e**, **3f**, and **3g** compare favorably with those reported for other structurally characterized alkynes FcC≡CAr, where Ar is an aryl group.[20,21] An inspection of the data listed in Table 1 reveals only negligible influence of the substituent at the aryl moiety on the geometric parameters. The minor differences observed are usually of no statistical significance and can be attributed to crystal packing effects. In all cases, the bonds connecting the alkyne moiety to the ferrocenyl and phenylene groups are noticeably shorter than the ordinary single bond because of extensive conjugation between the π systems.

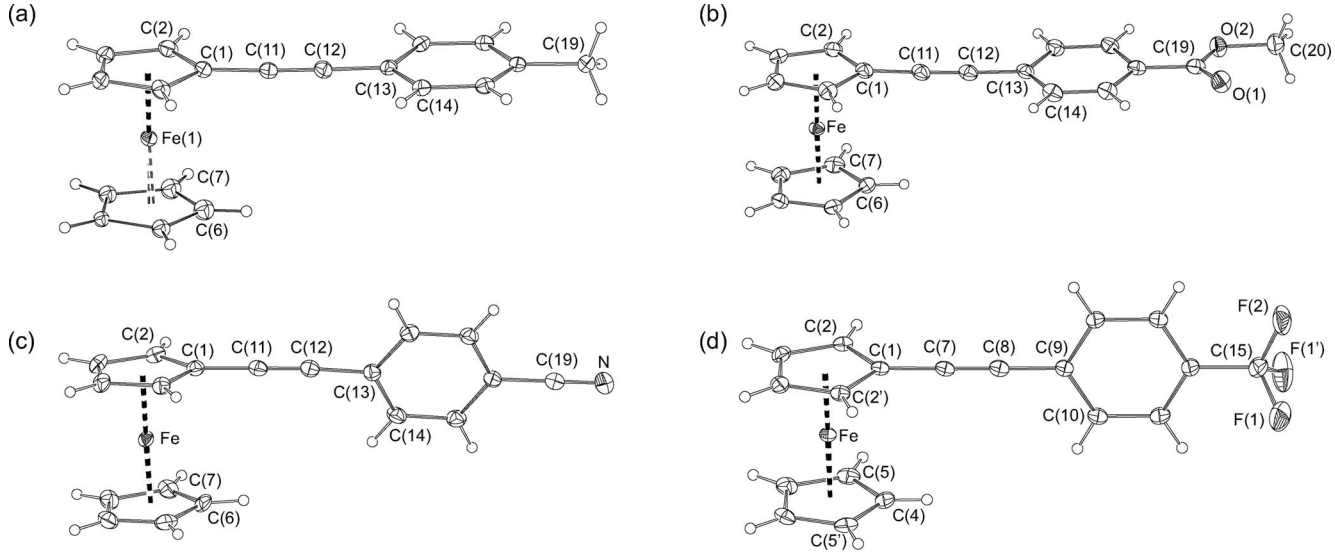

Figure 1. PLATON plots of (a) **3b** (molecule 1), (b) **3e**, (c) **3g**, and (d) **3f** showing displacement ellipsoids at the 30% probability level. The ring carbon atoms are labeled consecutively, and hence, only the labels for the pivotal atoms and the atoms adjacent to them are shown to avoid complicating the figures. Atomic labels in molecule 2 of **3b** are obtained by adding 20 to the respective atom labels in molecule 1 [except for Fe(2)]. For **3g**, only half of the molecule is structurally independent because of the imposed crystallographic symmetry (mirror plane).

Table 3. Selected geometric data for **3b**, **3e**, **3f**, and **3g** (in Å and °).[a]

Parameter	**3b** (mol. 1)	**3b** (mol. 2)	**3e**[c]	**3f**[d]	**3g**[e]
Fe–Cg(1)	1.647(2)	1.652(2)	1.644(1)	1.6424(8)	1.6419(8)
Fe–Cg(2)	–[b]	–[b]	1.646(1)	1.6513(9)	1.645(1)
∠Cp(1),Cp(2)	–[b]	–[b]	2.1(1)	0.2(1)	2.7(1)
FcC–C≡	1.432(4)	1.424(4)	1.427(3)	1.431(3)	1.435(2)
C≡C	1.200(4)	1.204(4)	1.198(3)	1.197(3)	1.193(3)
C–CC_6H_4	1.436(4)	1.438(4)	1.436(3)	1.436(3)	1.437(3)
FcC–C≡C	178.4(2)	177.2(3)	177.7(3)	179.3(2)	178.4(2)
C≡C–C_6H_4	176.7(2)	175.8(3)	177.2(2)	180.0(2)	176.7(2)
∠Cp1,Ph	1.0(2)	7.3(2)	2.9(1)	90	69.6(1)

[a] The ring planes are defined as follows: Cp(1) = C(1–5), Cp(2) = C(6–10), Ph = C(13–18). Cg(1) and Cg(2) are the centroids of the cyclopentadienyl rings Cp(1) and Cp(2), respectively. [b] Not reliable because of disorder of the unsubstituted cyclopentadienyl ring (see Experimental Section). [c] Further data: C(19)–O(1) 1.208(3), C(19)–O(2) 1.338(3), C(20)–O(2) 1.445(3), O(1)–C(19)–O(2) 123.4(2). [d] Further data: C(15)–F(1) 1.336(2), C(15)–F(2) 1.291(4), F(1)–C(15)–F(2) 107.6(2), F(1)–C(15)–F(1#) 102.5(2), # = *x*, 3/2 – *y*, *z*. [e] Further data: C(19)–N 1.147(3), C(16)–C(19)–N 179.3(2).

A notable difference can be seen in the mutual orientation of the phenylene and ferrocene moieties. Whereas the benzene rings in **3b** and **3e** deviate only slightly from the plane of their parent Cp(1) ring, those in **3g** and **3f** are mutually rotated by as much as 69.6(1)° and 90°, respectively. This, however, may reflect the presence of two mutually perpendicular π systems at the triple bond that are available for conjugation and would ideally give rise to two extreme, fully conjugated conformations having the aromatic rings either parallel with the Cp ring or rotated by 90°.

Compound **3b** crystallizes with the triclinic space group $P\bar{1}$ and has two molecules in the asymmetric unit. The remaining alkynes crystallize in monoclinic space groups, though with different symmetry. Whereas **3g** and **3e** form centrosymmetric crystal lattices, compound **3f** is chiral (space group $P2_1$). The molecule of **3f** resides on the crystallographic mirror plane so that the plane accommodates the benzene ring and the triple bond, and bisects the ferrocene and CF_3 units. A striking feature of the crystal assemblies is that the polar moieties (where present) do not exert any significant intermolecular contacts. The individual molecules of **3b** and **3e** associate predominantly through π···π stacking interactions[22] of their benzene rings with centroid···centroid distances close to the interplanar separation in α-graphite[23] and, additionally, through C–H···π interactions. On the other hand, **3e** and **3g** seem to form essentially molecular crystals, though with appropriately assembled molecular dipoles. In order to gain more insight into the role of the terminal substituents in the crystal assemblies, we have studied the electronic structure of the alkynes by computational methods.

Theoretical Calculations

The differences in the solid state arrangements can be explained already by examining the bonding relations in individual molecules. The most important feature – common to all of the four compounds – is the generation of a long-range interaction between the substituted cyclopentadienyl and phenylene rings. Should these two rings be (nearly) parallel, one of the acetylenic π systems is utilized as a mediator between the aromatic systems (Figure 2). Owing to this conjugation, the σ-bonds adjacent to the triple bond gain some surplus π character.

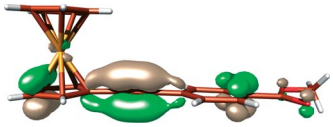

Figure 2. Orbital 77 of **3e** shown at the 5% probability level.

The conjugation depicted above involves the partially antibonding (though still occupied) orbitals on the connected aromatic rings. Although the fully bonding π orbitals of both rings are also properly shaped to generate an analogous interaction, no significant mixing with the alkyne orbitals occurs because of the large energy separation between them (Figure 3).

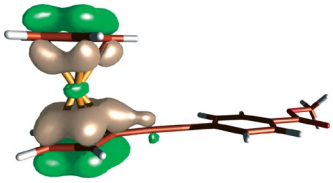

Figure 3. Orbital 64 of **3e** (5% probability) represents the practically unchanged (originally a_1) orbital of the ferrocene unit.

Since orbital 77 is generated by an attractive interaction in the $C_5H_4C{\equiv}CC_6H_4$ system, two corresponding partially bonding/antibonding orbitals and one fully antibonding (virtual) orbital are also formed (Figure 4).

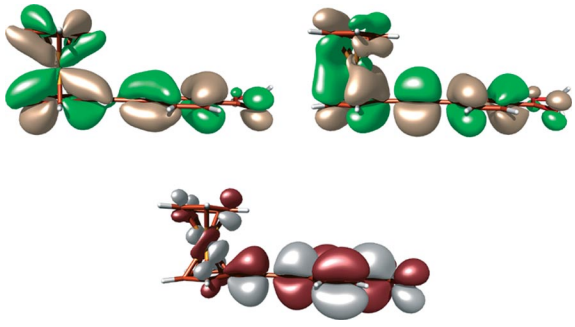

Figure 4. Orbitals 79 (top left), 86 (top right) and 90 (bottom) of **3e** (all at the 2% probability level). The two partially bonding/antibonding 79 and 86 and the completely antibonding 90 are partners to orbital 77; orbital 90 is the LUMO.

The stabilization in the solid state was examined for the molecular pair **3e**···**3e** at positions obtained from X-ray diffraction analysis. Since the electrostatic potential did not justify a dominant role of electrostatic interactions for **3e**···**3e** (see below), an alternative model based on covalent

stabilization was adopted. The only significant attractive intermolecular interaction was found in orbital 161 of the dimer (Figure 5).

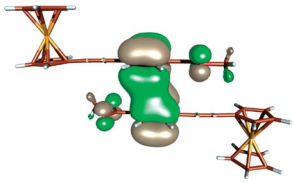

Figure 5. Orbital 161 of the **3e**···**3e** dimer (2% probability level).

As it is evident from the orbital shape, the intermolecular π···π interaction is affected by the second (originally degenerate) benzene orbital. Although the best overlap of such orbitals would occur without any shift, the encountered lateral displacement is a compromise between π···π attractive and repulsive interactions of several π-like molecular orbitals, in accordance with the dipolar model proposed by Hunter and Sanders.[24]

The rotation of the phenylene ring by 90° must clearly pick a different mechanism for the conjugation to be achieved. Alternatively, the perpendicular arrangement (observed for **3f** and **3g**) makes use of the conjugation via *both* acetylenic π systems, as demonstrated by orbitals 80 and 81 for **3f** (Figure 6). The partially antibonding counterparts of these orbitals are depicted in Figure 7.

Figure 6. Orbitals 80 (left) and 81 (right) for **3f** (5% probability level) responsible for conjugation of the perpendicular aromatic rings.

Figure 7. Orbitals 86 (left) and 87 (right; both at 5% probability level) for **3f**.

In contrast to the parallel arrangement, the perpendicular setting offers some additional stabilization, since the interaction between the phenylene ring and the C≡C bridge lacks any substantial antibonding interaction with the ferrocene unit (cf. orbitals 79 and 86 in Figure 4). Consequently, the originally e_{1g} benzene orbitals decrease in energy and are less prone to enter intermolecular interactions.

Lacking any significant π···π stacking interactions, the crystal assemblies of **3f** and **3g** are governed predominantly by dipolar interactions. The electrostatic potential, which is most negative at the terminal electron-withdrawing groups, supports this assumption. By contrast, the molecule of **3b** forming π···π stacked aggregates does not exhibit any significant electrostatic minima. Likewise, the most negative values of the electrostatic potential for **3e** are found on the carboxylic oxygen atoms (lone pairs).

Electrochemistry

Having the series of (arylethynyl)ferrocenes **3a**–**3g** in hand, we decided to study their electrochemical behavior by cyclic and differential pulse voltammetry at a platinum disc electrode in dichloromethane. A representative cyclic voltammogram is shown in Figure 8, and the potentials are given in Table 4.

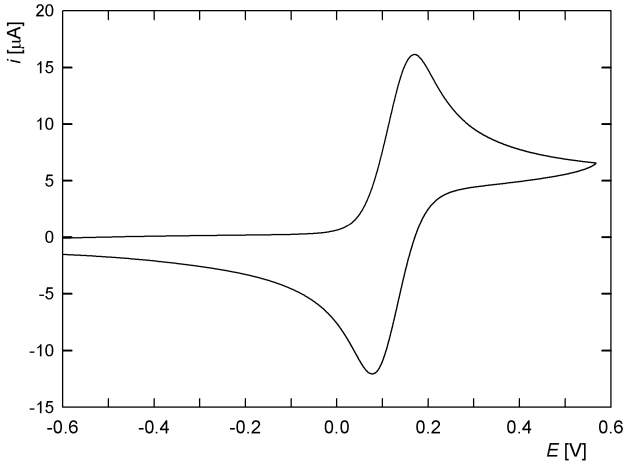

Figure 8. Cyclic voltammogram of **3d** as recorded in CH_2Cl_2 solution at a Pt-disc electrode and 0.1 Vs^{-1} scan rate. The potential scale is referenced to the ferrocene/ferrocenium couple.

Table 4. Summary of the electrochemical data.[a]

Ferrocene **3**	R	$E°'$ [V]	σ_p(R)[b]
3a	OMe	+0.090	–0.28
3b	Me	+0.100	–0.14
3c	H	+0.115	0
3d	Ph	+0.115	+0.02
3e	COOMe	+0.145	+0.44
3f	CF_3	+0.150	+0.53
3g	CN	+0.160	+0.71

[a] Recorded in CH_2Cl_2 at a Pt disc electrode. The potentials are given relative to the ferrocene/ferrocenium reference. $E°'$ was calculated as the mean of the anodic and cathodic peak potentials in cyclic voltammetry: $E°' = ½ (E_{pa} + E_{pc})$. [b] The σ_p-constants were taken from ref.[25]

The redox properties of the alkynes are very similar, and the voltammograms show single reversible oxidation attributable to the ferrocene/ferrocenium couple. In all cases, the redox wave occurs at a more positive value than that for unsubstituted ferrocene, which corresponds with the electron-withdrawing nature of the phenylethynyl group (σ_p = 0.16).[25] However, the exact position of the wave changes with the substituent at the phenyl ring. As evidenced by the data in Table 2, the electron-donating groups make the oxidation easier, while the electron-withdrawing groups increase the redox potential. This trend can be better illustrated by the linear free-energy correlation between the po-

tential of the ferrocene/ferrocenium oxidation and Hammett σ_p constants of the substituents (Figure 9). Although the absolute difference of the redox potentials is only 70 mV, their good correlation with σ_p indicates that the phenylethynyl moiety efficiently conveys the electronic influence of the *remote* modifying group, which corresponds with the observations made in the series of phenyl-[26,27] and (2-phenylethenyl)-substituted[27,28] ferrocenes.

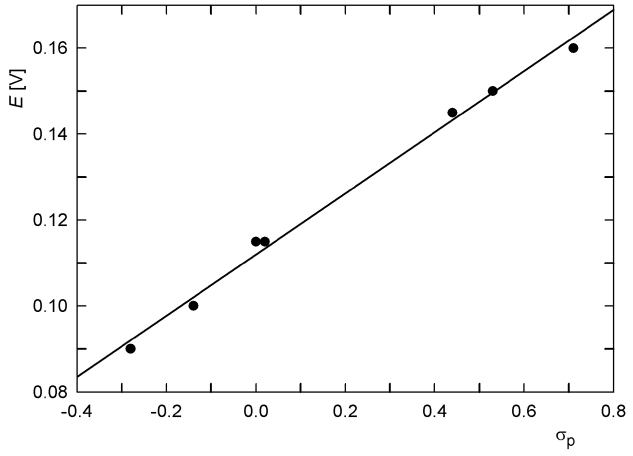

Figure 9. Linear free-energy relationship (LFER) between the redox potential of the ferrocene/ferrocene oxidation of **3a**–**3g** and the Hammett σ_p constants. Parameters of the fit: $E^{\circ\prime} = 0.071(3)\ \sigma_p + 0.112(1)$, $R^2 = 0.993$.

Conclusions

We have demonstrated that the cross metathesis of (prop-1-yn-1-yl)ferrocene with alkynes in the presence of a simple catalytic system comprising [$Mo(CO)_6$] and halophenols (modified Mortreux system) offers an alternative synthetic approach to substituted alkynylferrocenes. The reaction proceeds well with both aryl- and alkylpropynes to give the corresponding products in good yields and in reasonable selectivities, tolerating many functional substituents. In addition, the study showed that the metathesis reaction takes place with a wide array of halophenols with pK_A values in the range 4.9–9.9, which clearly indicates that the course of the reaction does not depend strictly on the acidity of the phenol OH group.

Structural data collected for the representative arylferrocenylalkynes, in conjunction with the results of DFT calculations, suggest extensive conjugation of the present π systems. This observation is in line with electrochemical data for 4-$XC_6H_4C{\equiv}CFc$, indicating a good electronic communication between the ferrocene unit and the remote modifying group R.

Experimental Section

General Comments: Mo-catalyzed reactions were performed under an atmosphere of dry argon by using vacuum-line, standard microwave vials and Schlenk techniques. Catalysts, phenols, toluene, and the other reagents used were obtained from commercial suppliers (Aldrich or Fluka) and were used without further purification. Dichloromethane and chloroform were dried with CaH_2 and distilled under argon before use. NMR spectra were recorded with a Varian UNITY 300 INOVA or Varian UNITY 400 INOVA instrument at 300 or 400 MHz (^1H) and 75 or 100 MHz (^{13}C) as solutions in C_6D_6 and are referenced to the residual solvent signal. Infrared spectra were recorded with a Bruker IFS 55 instrument with the ATR technique. HR mass spectra were recorded with a ZAB-SEQ (VG Analytical) spectrometer by using EI. Melting points (uncorrected) were determined with a Kofler apparatus. TLC was performed on silica gel 60 F_{254}-coated aluminum sheets (Merck). Column chromatography was performed on a preparative silica gel (63–200 μm) column. Electrochemical measurements were carried out with a computer-controlled multipurpose polarograph μAUTOLAB III (Eco Chemie, Netherlands) at room temperature by using a standard three-electrode cell with a rotating platinum disc electrode (AUTOLAB RDE, 3 mm diameter) as the working electrode, a platinum sheet auxiliary electrode, and a Ag/AgCl (3 M KCl) reference electrode. The compounds were dissolved in dichloromethane (Fluka, absolute, declared H_2O content <0.005%) to give a solution containing 1 mM of the analyte and 0.1 M Bu_4NPF_6 (Fluka, purissimum for electrochemistry). The solutions were deaerated with argon prior to the measurement and then kept under an argon blanket. The redox potentials are given relative to the ferrocene/ferrocenium reference, which was recorded before and after each measurement.

Starting Materials: The synthesis of 1-ferrocenylprop-1-yne (**1**) and diferrocenylethyne (**4**) were performed according to the previously reported methods, and their spectral characteristics were in agreement with previously reported data.[17] 1-Methoxy-4-(1-propyn-1-yl)benzene (**2a**), 1-methyl-4-(1-propyn-1-yl)benzene (**2b**), methyl 4-(1-propyn-1-yl) benzoate (**2e**), 1-(1-propyn-1-yl)-4-(trifluoromethyl)benzene (**2f**), 4-(1-propyn-1-yl)benzonitrile (**2g**), 2-(prop-1-yn-1-yl)pyridine (**2j**), 2-(prop-1-yn-1-yl)thiophene (**2k**), and 3-(prop-1-yn-1-yl)furan (**2l**) were prepared by Sonogashira coupling of the corresponding aryl halides with propyne.[29] 4-(Prop-1-yn-1-yl)biphenyl (**2d**) was prepared by lithiation of commercial 4-(ethynyl)-biphenyl with *n*BuLi followed by reaction with MeI in analogy to the synthesis of **1**. Pent-3-yn-1-yl acetate (**2i**) was prepared by reaction of pent-3-en-1-ol with acetyl chloride and Et_3N in dichloromethane.

General Procedure for Mo-Catalyzed Metathesis of 1-Ferrocenylprop-1-yne: Reactions were performed under an argon atmosphere in dried microwave vials. To a solution of 1-ferrocenylprop-1-yne (**1**) (112 mg, 0.5 mmol) in dry toluene (3 mL) was added [$Mo(CO)_6$] (13.2 mg, 0.05 mmol), 2-fluorophenol (56 mg, 45 μL, 1 mmol), and the appropriate propynyl derivative (1 mmol). The reaction mixture was heated to 120–130 °C until no further progress of the reaction was observed (2–24 h). The course of the reaction was monitored by TLC. The reaction mixture was then quenched with NaOH (1 M), and washed with dichloromethane (3 × 50 mL). The combined organic fractions were washed with water (50 mL), brine (50 mL), and dried with $MgSO_4$. The volatiles were removed under reduced pressure and column chromatography of the residue on silica gel (hexane/chloroform) afforded the products.

[(4-Methoxyphenyl)ethynyl]ferrocene (3a): 1-Methoxy-4-(1-propyn-1-yl)benzene (**2a**) (146 mg, 1 mmol); reaction time 5 h. Column chromatography (5:1 hexane/$CHCl_3$) afforded 98 mg (62%) of the title compound as an orange solid: m.p. 124–125 °C (EtOH). ^1H NMR (400 MHz, C_6D_6): δ = 3.18 (s, 3 H), 3.93–3.96 (m, 2 H), 4.11

(s, 5 H), 4.48–4.51 (m, 2 H), 6.57–6.62 (m, 2 H), 7.47–7.52 (m, 2 H) ppm. ^{13}C NMR (100 MHz, C_6D_6): δ = 55.4, 67.3, 69.7 (2 C), 71.0 (5 C), 72.4 (2 C), 87.2, 88.1, 115.1 (2 C), 117.4 133.8 (2 C), 160.4 ppm. IR (neat): $\tilde{\nu}$ = 3097, 2992, 2959, 2923, 2830, 1901, 1607, 1515, 1258, 1105, 1027, 830 cm^{-1}. UV/Vis (hexane): λ_{max} (ε, M^{-1} cm^{-1}) = 446 (2926) nm. HRMS (*m*/*z*): calcd. for $C_{19}H_{16}FeO$ 316.05506; found 316.05482. $C_{19}H_{16}OFe$ (316.17): calcd. C 72.17, H 5.10; found C 72.04, H 5.20. R_f (5:1 hexane/$CHCl_3$) = 0.28.

[(4-Methylphenyl)ethynyl]ferrocene (3b): 1-Methyl-4-(1-propyn-1-yl)benzene (**2b**) (130 mg, 1 mmol); reaction time 3 h. Column chromatography (5:1 hexane/$CHCl_3$) afforded 63 mg (42%) of the title compound as a red needles: m.p. 95–97 °C (EtOH). ^{1}H NMR (300 MHz, C_6D_6): δ = 1.98 (s, 3 H), 3.92–3.96 (m, 2 H), 4.09 (s, 5 H), 4.46–4.50 (m, 2 H), 6.80–6.85 (m, 2 H), 7.46–7.52 (m, 2 H) ppm. ^{13}C NMR (75 MHz, C_6D_6): δ = 21.9, 66.7, 69.8 (2 C), 70.9 (5 C), 72.5 (2 C), 89.0, 122.4, 130.1 (2 C), 132.4 (2 C), 138.4 ppm. IR (neat): $\tilde{\nu}$ = 2956, 2920, 2848, 1515, 1461, 1410, 1374, 1260, 1186, 1105, 1024, 923, 815, 680 cm^{-1}. UV/Vis (hexane): λ_{max} (ε, M^{-1} cm^{-1}) = 450 (1143) nm. HRMS (*m*/*z*): calcd. for $C_{19}H_{16}Fe$ 300.06014; found 300.06050. $C_{19}H_{16}Fe$ (300.18): calcd. C 76.05, H 5.35; found C 76.28, H 5.51. R_f (5:1 hexane/$CHCl_3$) = 0.18.

(Phenylethynyl)ferrocene (3c): (1-Propyn-1-yl)benzene (**2c**) (116 mg, 1 mmol), reaction time 5 h. Column chromatography (5:1 hexane/$CHCl_3$) afforded 90 mg (63%) of the title compound as a red solid. UV/Vis (hexane): λ_{max} (ε, M^{-1} cm^{-1}) = 464 (3737) nm. The spectroscopic data were in agreement with the previously reported ones.[30]

[(1,1′-Biphenyl-4-yl)ethynyl]ferrocene (3d): 4-(Prop-1-yn-1-yl)-1,1′-biphenyl (**2d**) (192 mg, 1 mmol), reaction time 4 h. Column chromatography (9:1 hexane/$CHCl_3$) afforded 107 mg (59%) of the title compound as an orange solid: m.p. 143–144 °C (EtOH). ^{1}H NMR (400 MHz, C_6D_6): δ = 3.94–3.98 (m, 2 H), 4.11 (s, 5 H), 4.50–4.54 (m, 2 H), 7.10–7.22 (m, 4 H), 7.28–7.39 (m, *J* = Hz, 4 H) 7.57–7.64 (m, 1 H) ppm. ^{13}C NMR (100 MHz, C_6D_6): δ = 66.7, 69.9 (2 C), 71.0 (5 C), 72.5 (2 C), 87.2, 90.6, 124.2, 128.0 (2 C), 128.1, 128.2 (2 C), 129.7 (2 C), 132.8 (2 C), 133.1, 141.44 ppm. IR (neat): $\tilde{\nu}$ = 3097, 3025, 2956, 2923, 2851, 2223, 1909, 1488, 1446, 1407, 1105, 1006, 842, 767, 704 cm^{-1}. UV/Vis (hexane): λ_{max} (ε, M^{-1} cm^{-1}) = 450 (4143) nm. HRMS (*m*/*z*): calcd. for $C_{24}H_{18}Fe$ 362.07579; found 362.07510. $C_{24}H_{18}Fe$ (362.24): calcd. C 79.60, H 4.98; found C 79.24, H 5.20. R_f (9:1 hexane/$CHCl_3$) = 0.28.

Methyl 4-[(Ferrocenyl)ethynyl] Benzoate (3e): Methyl 4-(1-propyn-1-yl) benzoate (**2e**) (174 mg, 1 mmol), reaction time 5 h. Column chromatography (5:1 hexane/$CHCl_3$) afforded 93 mg (54%) of the title compound as an orange solid: m.p. 154–155 °C (EtOH). ^{1}H NMR (400 MHz, C_6D_6): δ = 3.45 (s, 3 H), 3.93–3.97 (m, 2 H), 4.07 (s, 5 H), 4.45–4.48 (m, 2 H), 7.39–7.45 (m, 2 H), 7.94–7.99 (m, 2 H) ppm. ^{13}C NMR (100 MHz, C_6D_6): δ = 52.3, 65.8, 70.2 (2 C), 71.0 (5 C), 72.6 (2 C), 86.7, 93.3, 129.7, 130.3 (2 C), 132.2 (2 C), 166.8 ppm. IR (neat): $\tilde{\nu}$ = 3085, 3016, 2950, 2206, 1936, 1724, 1604, 1431, 1404, 1273, 1108, 962, 926, 830, 767, 695 cm^{-1}. UV/Vis (hexane): λ_{max} (ε, M^{-1} cm^{-1}) = 450 (2868) nm. HRMS (*m*/*z*): calcd. for $C_{20}H_{16}FeO_2$ 344.04997; found 344.04951. $C_{20}H_{16}O_2Fe$ (344.18) calcd. C 69.79, H 4.69, found C 69.31, H 4.49. R_f (5:1 hexane/$CHCl_3$) = 0.50.

{[4-(Trifluoromethyl)phenyl]ethynyl}ferrocene (3f): 1-(1-Propyn-1-yl)-4-(trifluoromethyl)benzene (**2f**) (184 mg, 1 mmol); reaction time 7 h. Column chromatography (25:1 hexane/$CHCl_3$) afforded 57 mg (32%) of the title compound as an orange solid: m.p. 127–128 °C (EtOH). ^{1}H NMR (300 MHz, C_6D_6): δ = 3.93–3.97 (m, 2 H), 4.07 (s, 5 H), 4.44–4.48 (m, 2 H), 7.11–7.18 (m, 2 H) overlapping with the C_6D_6 signal, 7.24–7.31 (m, 2 H) ppm. ^{13}C NMR (75 MHz, C_6D_6): δ = 30.9, 65.5, 70.3 (2 C), 71.1 (5 C), 72.7 (2 C), 85.9, 92.8, 126.1 (2 C), 126.3 (2 C), 132.4 ppm. IR (neat): $\tilde{\nu}$ = 3097, 3076, 2956, 2920, 2851, 2226, 1933, 1733, 1616, 1464, 1401, 1323, 1171, 1108, 1072, 1012, 848, 824, 743 cm^{-1}. HRMS (*m*/*z*): calcd. for $C_{19}H_{13}F_3Fe$ 354.03188; found 354.03101. R_f (25:1 hexane/$CHCl_3$) = 0.54.

[(4-Cyanophenyl)ethynyl]ferrocene (3g): 4-(1-Propyn-1-yl)benzonitrile (**2g**) (141 mg, 1 mmol); reaction time 4 h. Column chromatography (5:1 hexane/$CHCl_3$) afforded 52 mg (33%) of the title compound as orange needles; m.p.: 171–172 °C (EtOH). ^{1}H NMR (400 MHz, C_6D_6): δ = 3.92–3.99 (m, 2 H), 4.05 (s, 5 H), 4.40–4.48 (m, 2 H), 6.78 (d, *J* = 8.0 Hz, 2 H), 7.03–7.07 (m, 2 H) ppm. ^{13}C NMR (100 MHz, C_6D_6): δ = 65.1, 70.4 (2 C), 71.1 (5 C), 72.7 (2 C), 85.9, 94.7, 112.0, 119.2, 129.2, 132.3 (2 C), 132.7 (2 C) ppm. IR (neat): $\tilde{\nu}$ = 3097, 2953, 2923, 2851, 2220, 2199, 1936, 1598, 1502, 1407, 1270, 1159, 1102, 1003, 845 cm^{-1}. UV/Vis (hexane): λ_{max} (ε, M^{-1} cm^{-1}) = 450 (2695) nm. HRMS (*m*/*z*): calcd. for $C_{19}H_{13}FeN$ 311.03974; found 311.04053. $C_{19}H_{13}FeN$ (311.17): calcd. C 73.33, H 4.21, N 4.50; found C 72.68, H 4.36, N 4.03. R_f (5:1 hexane/$CHCl_3$) = 0.22.

(2-Heptyn-1-yl)ferrocene (3h): Oct-2-yne (**2h**) (110 mg, 1 mmol), reaction time 5 h. Column chromatography (6:1 hexane/$CHCl_3$) afforded 94 mg (64%) of the title compound as a dark brown oil. ^{1}H NMR (400 MHz, C_6D_6): δ = 0.81 (t, *J* = 7.2 Hz, 3 H), 1.17 (q, *J* = 7.2 Hz, 2 H), 1.26–1.38 (m, 2 H), 1.43 (kv, *J* = 6.6 Hz, 2 H), 2.18 (t, *J* = 6.9 Hz, 2 H), 3.88–3.91 (m, 2 H), 4.10 (s, 5 H), 4.40–4.42 (m, 2 H) ppm. ^{13}C NMR (100 MHz, C_6D_6): δ = 14.8, 20.6, 23.2, 29.7, 32.1, 68.2, 69.2 (2 C), 70.8 (5 C), 72.3 (2 C), 79.7, 87.3 ppm. IR (neat): $\tilde{\nu}$ = 3097, 2956, 2926, 2857, 1712, 1464, 1258, 1204, 1108, 1057, 1024, 1000, 821, 728 cm^{-1}. HRMS: *m*/*z* calcd. for $C_{17}H_{20}Fe$ 280.09144; found 280.09175. R_f (6:1 hexane/$CHCl_3$) = 0.24.

4-(Ferrocenyl)but-3-yn-1-yl Acetate (3i): Pent-3-yn-1-yl acetate (**2i**) (126 mg, 1 mmol), reaction time 10 h. Column chromatography (5:1 hexane/$CHCl_3$) afforded 40 mg (27%) of the title compound as a dark red oil. ^{1}H NMR (400 MHz, C_6D_6): δ = 1.65 (s, 3 H), 2.35 (t, *J* = 5.1 Hz, 2 H), 3.87–3.90 (m, 2 H), 4.03–4.08 (m, 2 H) (overlapping with the OCH_2 signal), 4.07 (s, 5 H), 4.35–4.39 (m, 2 H) ppm. ^{13}C NMR (100 MHz, C_6D_6): δ = 21.0, 68.1, 69.3 (2 C), 70.9 (5 C), 72.4 (2 C), 81.1, 82.1, 170.5 ppm. IR (neat): $\tilde{\nu}$ = 3096, 2961, 2924, 2851, 2233, 1741, 1727, 1459, 1383, 1363, 1239, 1039, 1003, 817 cm^{-1}. HRMS (*m*/*z*): calcd. for $C_{16}H_{16}FeO_2$ 296.04997; found 296.05010. R_f (5:1 hexane/$CHCl_3$) = 0.20.

General Procedure for Cross-Metathesis of 1 with 2e in the Presence of Various Phenols: To a solution of **1** (56 mg, 0.25 mmol) in dry toluene (3 mL) was added [$Mo(CO)_6$] (6.6 mg, 0.025 mmol), phenol (0.25 mmol), and **2e** (87 mg, 0.5 mmol). The reaction mixture was heated to 130 °C for 8 h and then quenched with NaOH (2 M) and washed with dichloromethane (2 × 20 mL). The combined organic fractions were washed with H_2O (50 mL), brine (50 mL), and dried with $MgSO_4$. The volatiles were removed under reduced pressure and column chromatography of the residue on silica gel (4:1 hexane/chloroform) afforded **3e**.

1. Reaction in the Presence of 4-Fluorophenol: 4-Fluorophenol (28 mg, 0.25 mmol). Chromatography afforded 54 mg (63%) of **3e**, 5 mg (6%) of **1**, and 7 mg (7%) of **2**.

2. Reaction in the Presence of 4-Chlorophenol: 4-Chlorophenol (32 mg, 0.25 mmol). Chromatography afforded 42 mg (49%) of **3e** and 4 mg (5%) of **2**.

3. Reaction in the Presence of 2-Fluorophenol: 2-Fluorophenol (28 mg, 45 μL, 0.25 mmol). Chromatography afforded 47 mg (54%) of **3e**, 3 mg (3%) of **1**, and 6 mg (6%) of **2**.

4. Reaction in the Presence of 3-Nitrophenol: 3-Nitrophenol (35 mg, 0.25 mmol). Formation of **3e** and **2** was not observed. The starting material remained unchanged.

5. Reaction in the Presence of 2-Chlorophenol: 2-Chlorophenol (32 mg, 26 μL, 0.25 mmol). Chromatography afforded 53 mg (62%) of **3e**, 3 mg (4%) of **1**, and 6 mg (8%) of **2**.

6. Reaction in the Presence of 2,4-Dichlorophenol: 2,4-Dichlorophenol (40 mg, 0.25 mmol). Chromatography afforded 42 mg (48%) of **3e** and 5 mg (6%) of **1**.

7. Reaction in the Presence of 2-Nitrophenol: 2-Nitrophenol (35 mg, 0.25 mmol). Formation of **3e** and **2** was not observed. The starting material remained unchanged.

8. Reaction in the Presence of 4-Nitrophenol: 4-Nitrophenol (35 mg, 0.25 mmol). Formation of **3e** and **2** was not observed. The starting material remained unchanged.

9. Reaction in the Presence of 2,4,5-Trichlorophenol: 2,4,5-Trichlorophenol (52 mg, 0.25 mmol). Chromatography afforded 42 mg (48%) of **3e** and 3 mg (3%) of **2**.

10. Reaction in the Presence of 2,3,4,5,6-Pentafluorophenol: 2,3,4,5,6-Pentafluorophenol (46 mg, 0.25 mmol). Chromatography afforded 69 mg (80%) of **3e** and 5 mg (6%) of **2**.

11. Reaction in the Presence of 2,3,4,5,6-Pentachlorophenol: 2,3,4,5,6-Pentachlorophenol (66 mg, 0.25 mmol). Chromatography afforded 39 mg (45%) of **3e** and 9 mg (3%) of **2**.

X-ray Crystallography: All crystals used for single-crystal X-ray diffraction analysis were grown from ethanol (**3b**: orange plate, $0.05 \times 0.16 \times 0.30$ mm^3, **3e**: red plate, $0.04 \times 0.50 \times 0.58$ mm^3, **3g**: orange needle, $0.12 \times 0.12 \times 0.50$ mm^3, **3f**: orange block, $0.35 \times 0.45 \times 0.60$ mm^3). Full-set diffraction data ($\pm h \pm k \pm l$, $2\theta \leq$ 54–55°) were collected with a Nonius KappaCCD diffractometer equipped with a Cryostream Cooler (Oxford Cryosystems) using graphite monochromatized Mo-K_α radiation (λ = 0.71073 Å) and analyzed with the HKL program package.[31] The data for **3e** and **3g** were corrected for absorption. The ranges of the transmission factors are given in Table 5.

The structures were solved by direct methods (SIR97[32]) and refined by the full-matrix least-squares procedure on F^2 (SHELXL97[33]). The unsubstituted cyclopentadienyl in both structurally independent molecules of **3b** are disordered and were modeled as if contributed by two orientations. The components were refined independently with isotropic displacement parameters, which led to fractional occupancies of ca. 28:72. All other non-hydrogen atoms were refined with anisotropic displacement parameters. The hydrogen atoms were included in the calculated positions and refined as riding atoms. Relevant crystallographic data are given in Table 5. Geometric parameters and structural drawings were obtained by using a recent version of the Platon program.[34]

CCDC-667781 (**3b**), -667782 (**3e**), -667783 (**3g**), and -667784 (**3f**) contain the supplementary crystallographic data for this paper. These data can be obtained free of charge from The Cambridge Crystallographic Data Centre via www.ccdc.cam.ac.uk/data_request/cif.

Computational Details: Computational studies have been performed on the Bohr Cluster located at the J. Heyrovský Institute of Physical Chemistry, Academy of Sciences of the Czech Republic, by using Gaussian 03, Revision C.02.[35] DFT results were obtained by carrying out spin-restricted calculations by utilizing Becke's 1988 exchange functional[36] and the Perdew-Wang 91 gradient-corrected correlation functional[37] (BPW91). The numerical integration grid consisted of a pruned grid with 99 radial shells each with 590 angular points. Calculations utilized the Douglas–Kroll–Hess 2nd order scalar relativistic Hamiltonian[38] and the 6-311++G(d,p) basis set employed for all atoms. All input geometries were those obtained from the diffraction experiments; their computational optimization was not attempted. Orbital numberings are given according to their increasing energy. Natural Bonding Analysis

Table 5. Crystallographic and collection data and structure refinement parameters for **3b**, **3e**, **3g**, and **3f**.[a]

Compound	**3b**	**3e**	**3g**	**3f**
Formula	$C_{19}H_{16}Fe$	$C_{20}H_{16}FeO_2$	$C_{19}H_{13}FeN$	$C_{19}H_{13}F_3Fe$
M [g mol^{-1}]	300.17	344.18	311.15	354.14
Crystal system	triclinic	monoclinic	monoclinic	monoclinic
Space group	$P\bar{1}$ (no. 2)	$P2_1/c$ (no. 14)	$P2_1$ (no. 4)[g]	$P2_1/m$ (no. 11)
a [Å]	7.5552(2)	7.4731(2)	9.6748(4)	7.6412(2)
b [Å]	10.8247(4)	18.5749(4)	7.3107(2)	8.7141(2)
c [Å]	17.7486(5)	11.4966(3)	10.1676(4)	11.5452(3)
α [°]	80.192(2)			
β [°]	79.539(2)	108.077(1)	98.704(2)	97.432(2)
γ [°]	89.744(2)			
V [Å^3]	1406.02(8)	1517.10(7)	710.87(4)	762.29(3)
Z	4	4	2	2
$D_{calcd.}$ [g mL^{-1}]	1.418	1.507	1.454	1.543
μ(Mo-K_α) [mm^{-1}]	1.058	1.001[f]	1.051[h]	1.016
Diffractions total	22106	21754	11825	11780
Unique/obsd.[b] diffractions	6180/4693	3339/2893	3262/3066	3472/3315
R_{int} [%][c]	2.18	4.62	4.25	2.6
R (observed data) [%] [b,d]	5.15	3.64	2.34	3.10
R, wR (all data) [%][d]	7.08, 13.7	4.42, 9.59	2.73, 5.26	3.21, 8.05
$\Delta\rho$ [e Å^{-3}]	1.80,[e] –0.50	1.67,[e] –0.33	0.22, –0.31	0.66, –0.52

[a] Common details: T = 150(2) K. [b] Diffractions with $I_o > 2\sigma(I_o)$. [c] $R_{int} = \Sigma|F_o^2 - F_o^2(\text{mean})|/\Sigma F_o^2$, where F_o^2(mean) is the average intensity of symmetry-equivalent diffractions. [d] $R = \Sigma||F_o| - |F_c||/\Sigma|F_o|$, $wR = [\Sigma\{w(F_o^2 - F_c^2)^2\}/\Sigma\, w(F_o^2)^2]^{1/2}$. [e] The residual electron density probably reflects the crystal shape (thin plates) and possible defects due to layered structure. [f] The range of transmission coefficients: 0.787–0.970. [g] Flack's parameter = 0.03(1). [h] The range of transmission coefficients: 0.682–0.899.

(NBO) was carried out against the final wavefunctions by using the Natural Bond Analysis[39] program integrated in Gaussian. Contour diagrams of the molecular orbitals were obtained with Molden.[40]

Supporting Information (see footnote on the first page of this article): Calculated orbital energies and orbital diagrams for **3b** and **3e**–**g** and spectroscopic data for all prepared compounds.

Acknowledgments

We gratefully acknowledge financial support by the Ministry of Education of the Czech Republic (project Nos.. LC06070 and MSM 0021620857) and from the Grant Agency of the Czech Republic (project no. 203/05/0276).

[1] For reviews see: a) Y. Chauvin, *Angew. Chem. Int. Ed.* **2006**, *45*, 3741–3747; b) R. R. Schrock, *Angew. Chem. Int. Ed.* **2006**, *45*, 3748–3757; c) R. H. Grubbs, *Angew. Chem. Int. Ed.* **2006**, *45*, 3760–3765; d) D. Astruc, *New J. Chem.* **2005**, *29*, 42–56; e) R. H. Grubbs, *Tetrahedron* **2004**, *60*, 7117–7140; f) A. Deiters, S. F. Martin, *Chem. Rev.* **2004**, *104*, 2199–2238; g) S. T. Diver, A. J. Giessert, *Chem. Rev.* **2004**, *104*, 1317–1382; h) R. R. Schrock, A. H. Hoveyda, *Angew. Chem. Int. Ed.* **2003**, *42*, 4592–4633; i) S. J. Connon, S. Blechert, *Angew. Chem. Int. Ed.* **2003**, *42*, 1900–1923; j) T. M. Trnka, R. H. Grubbs, *Acc. Chem. Res.* **2001**, *34*, 18–29; k) A. Fürstner, *Angew. Chem. Int. Ed.* **2000**, *39*, 3012–3043; l) R. H. Grubbs (Ed.), *Handbook of Metathesis*, Wiley-VCH, Weinheim, **2003**, vols. 1–3; m) A. Fürstner (Ed.), *Alkene Metathesis in Organic Synthesis*, Springer, Berlin, **1998**.

[2] For reviews see: a) U. H. F. Bunz, L. Kloppenburg, *Angew. Chem. Int. Ed.* **1999**, *38*, 478–481; b) U. H. F. Bunz, *Acc. Chem. Res.* **2001**, *34*, 998–1010; c) A. Fürstner, P. W. Davies, *Chem. Commun.* **2005**, *346*, 2307–2320; d) O. Coutelier, A. Mortreux, *Adv. Synth. Catal.* **2006**, *348*, 2038–2042; e) A. Mortreux, O. Coutelier, *J. Mol. Catal. A: Chem.* **2006**, *254*, 96–104; f) R. R. Schrock, C. Czekelius, *Adv. Synth. Catal.* **2007**, *349*, 55–77; g) W. Zhang, J. S. Moore, *Adv. Synth. Catal.* **2007**, *349*, 93–120; h) E. Groaz, D. Banti, M. North, *Adv. Synth. Catal.* **2007**, *349*, 142–146.

[3] a) A. Fürstner, O. Guth, A. Rumbo, G. Seidel, *J. Am. Chem. Soc.* **1999**, *121*, 11108–11113; b) A. Fürstner, K. Grela, *J. Am. Chem. Soc.* **2000**, *122*, 11799–11805; c) A. Fürstner, A. Rumbo, *J. Org. Chem.* **2000**, *65*, 2608–2611; d) A. Fürstner, K. Radkowski, J. Grabowski, C. Wirtz, R. Mynott, *J. Org. Chem.* **2000**, *65*, 8758–8762; e) A. Fürstner, G. Seidel, *J. Organomet. Chem.* **2000**, *606*, 75–78; f) A. Fürstner, C. Mathes, *Org. Lett.* **2001**, *3*, 221–223; g) A. Fürstner, C. Mathes, K. Grela, *Chem. Commun.* **2001**, 1057–1058; h) B. Aguilera, L. B. Wolf, P. Nieczypor, F. P. J. Rutjes, H. S. Overkleeft, J. C. M. van Hest, H. E. Schoemaker, B. Wang, J. C. Mol, A. Fürstner, M. Overhand, G. A. van der Marel, J. H. van Boom, *J. Org. Chem.* **2001**, *66*, 3584–3589; i) A. Fürstner, A.-S. Castanet, K. Radkowski, C. W. Lehmann, *J. Org. Chem.* **2003**, *68*, 1521–1528; j) M. IJsselstijn, B. Aguilera, G. A. van der Marel, J. H. van Boom, F. L. van Delft, H. E. Schoemaker, H. S. Overkleeft, F. P. J. T. Rutjes, M. Overhand, *Tetrahedron Lett.* **2004**, *45*, 4379–4382; k) N. Ghalit, A. J. Poot, A. Fürstner, D. T. S. Rijkers, R. M. J. Liskamp, *Org. Lett.* **2005**, *7*, 2961–2964.

[4] a) L. Kloppenburg, D. Song, U. H. F. Bunz, *J. Am. Chem. Soc.* **1998**, *120*, 7973–7974; b) L. Kloppenburg, D. Jones, U. H. F. Bunz, *Macromolecules* **1999**, *32*, 4194–4203; c) P.-H. Ge, W. Fu, W. A. Herrmann, E. Herdtweck, C. Campana, R. D. Adams, U. H. F. Bunz, *Angew. Chem. Int. Ed.* **2000**, *39*, 3607–3610; d) N. G. Pschirer, W. Fu, R. D. Adams, U. H. F. Bunz, *Chem. Commun.* **2000**, 87–88; e) G. Brizius, N. G. Pschirer, W. Steffen, K. Stitzer, H.-C. zur Loye, U. H. F. Bunz, *J. Am. Chem. Soc.* **2000**, *122*, 12435–12440; f) N. G. Pschirer, U. H. F. Bunz, *Macromolecules* **2000**, *33*, 3961–3963; g) W. Steffen, U. H. F. Bunz, *Macromolecules* **2000**, *33*, 9518–9521; h) N. G. Pschirer, A. R. Marshall, C. Stanley, H. W. Beckham, U. H. F. Bunz, *Macromol. Rapid Commun.* **2000**, *21*, 493–495; i) G. Brizius, S. Kroth, U. H. F. Bunz, *Macromolecules* **2002**, *35*, 5317–5319; j) W. Zhang, J. S. Moore, *J. Am. Chem. Soc.* **2004**, *126*, 12796; k) W. Zhang, J. S. Moore, *Macromolecules* **2004**, *37*, 3973–3975; l) W. Zhang, J. S. Moore, *J. Am. Chem. Soc.* **2005**, *127*, 11863–11870; m) W. Zhang, S. M. Brombosz, J. L. Mendoza, J. S. Moore, *J. Org. Chem.* **2005**, *70*, 10198–10201; n) C. A. Johnson II, Y. Lu, M. M. Haley, *Org. Lett.* **2007**, *9*, 3725–3728.

[5] E. B. Bauer, F. Hampel, J. A. Gladysz, *Adv. Synth. Catal.* **2004**, *346*, 812–822.

[6] a) A. Mortreux, M. Blanchard, *J. Chem. Soc., Chem. Commun.* **1974**, 786–787; b) A. Mortreux, N. Dy, M. Blanchard, *J. Mol. Catal.* **1975/1976**, *1*, 101–109; c) M. Petit, A. Mortreux, F. Petit, *J. Chem. Soc., Chem. Commun.* **1982**, 1385–1386.

[7] L. Kloppenburg, U. H. F. Bunz, *J. Organomet. Chem.* **2000**, *606*, 13–15.

[8] a) L. G. McCullogh, R. R. Schrock, J. C. Dewan, J. C. Murdzek, *J. Am. Chem. Soc.* **1985**, *107*, 5987–5998; b) Y.-C. Tsai, P. L. Diaconescu, C. C. Cummins, *Organometallics* **2000**, *19*, 5260–5262; c) W. Zhang, S. Kraft, J. S. Moore, *Chem. Commun.* **2003**, 832–833; d) J. M. Blackwell, J. S. Figueroa, F. H. Stephens, C. C. Cummins, *Organometallics* **2003**, *22*, 3351–3353; e) W. Zhang, S. Kraft, J. S. Moore, *J. Am. Chem. Soc.* **2004**, *126*, 329–335; f) R. L. Gdula, M. J. A. Johnson, *J. Am. Chem. Soc.* **2006**, *128*, 9614–9615; g) H. M. Cho, H. Weissman, S. R. Wilson, J. S. Moore, *J. Am. Chem. Soc.* **2006**, *128*, 14742–14743.

[9] a) R. R. Schrock, D. N. Clark, J. Sancho, J. H. Wengrovius, S. M. Rocklage, S. F. Pedersen, *Organometallics* **1982**, *1*, 1645–1651; b) R. R. Schrock, *Polyhedron* **1995**, *14*, 3177–3195; c) Z. J. Tonzetich, Y. C. Lam, P. Müller, R. R. Schrock, *Organometallics* **2007**, *26*, 475–477.

[10] a) Y.-C. Tsai, P. L. Diaconescu, C. C. Cummins, *Organometallics* **2000**, *19*, 5260–5262; b) A. Fürstner, C. Mathes, C. W. Lehmann, *J. Am. Chem. Soc.* **1999**, *121*, 9453–9454; c) C. C. Cummins, *Chem. Commun.* **1998**, 1777–1786; d) C. E. Laplaza, A. L. Odom, W. M. Davis, C. C. Cummins, J. D. Protasiewicz, *J. Am. Chem. Soc.* **1995**, *117*, 4999–5000.

[11] a) N. Kaneta, T. Hirai, M. Mori, *Chem. Lett.* **1995**, 627–628; b) N. Kaneta, K. Hikichi, S. Asaka, M. Uemura, M. Mori, *Chem. Lett.* **1995**, 1055–1056.

[12] N. G. Pschirer, U. H. F. Bunz, *Tetrahedron Lett.* **1999**, *40*, 2481–2484.

[13] a) K. Grela, J. Ignatowska, *Org. Lett.* **2002**, *4*, 3747–3749; b) V. Sashuk, J. Ignatowska, K. Grela, *J. Org. Chem.* **2004**, *69*, 7748–7751.

[14] D. Villemin, M. Héroux, V. Blot, *Tetrahedron Lett.* **2001**, *42*, 3701–3703.

[15] a) V. Huc, R. Weihofen, I. Martinez-Chimenez, P. Oulié, C. Lepetit, G. Lavigne, R. Chauvin, *New J. Chem.* **2003**, *27*, 1412–1414; b) V. Maraval, C. Lepetit, A.-M. Caminade, J.-P. Majoral, R. Chauvin, *Tetrahedron Lett.* **2006**, *47*, 2155–2159.

[16] a) M. Sato, M. Watanabe, *Chem. Commun.* **2002**, 1574–1575; b) M. Sato, Y. Kubota, Y. Kawata, T. Fujihara, K. Unoura, A. Oyama, *Chem. Eur. J.* **2006**, *12*, 2282–2292.

[17] M. Kotora, D. Nečas, P. Štepnička, *Collect. Czech. Chem. Commun.* **2003**, *68*, 1897–1903.

[18] a) W. L. Mock, L. A. Morsch, *Tetrahedron* **2001**, *57*, 2957–2964; b) J. Hine, K. Ahn, *J. Org. Chem.* **1987**, *52*, 2083–2086; c) D. Stefanidis, S. Cho, S. Dhe-Paganon, W. P. Jencks, *J. Am. Chem. Soc.* **1993**, *115*, 1650–1656; d) G. Cevasco, S. Thea, *J. Org. Chem.* **1998**, *63*, 2125–2129.

[19] a) D. N. Kravtsov, E. S. Shubina, L. M. Epshtein, V. M. Pachevskaya, *Izv. Akad. Nauk SSSR, Ser. Khim.* **1982**, *31*, 265–270; *Russ. Chem. Bull.* **1982**, *31*, 242–246; b) A. V. Golounin, V. A.

Sokolenko, O. V. Zakharova, E. A. Shor, M. S. Tovbis, *Russ. J. Appl. Chem.* **2007**, *80*, 887–890.

[20] S. Koecher, H. Lang, *J. Organomet. Chem.* **2001**, *637–639*, 198–203.

[21] Selected examples: a) R. P. Hsung, C. E. D. Chidsey, L. R. Sita, *Organometallics* **1995**, *14*, 4808–4815; b) J. T. Lin, J. J. Wu, C.-S. Li, Y. S. Wen, K. J. Lin, *Organometallics* **1996**, *15*, 5028–5034; c) H. Fink, N. J. Long, A. J. Martin, G. Opromolla, A. J. P. White, D. J. Williams, P. Zanello, *Organometallics* **1997**, *16*, 2646–2650; d) L. Cuffe, R. D. A. Hudson, J. F. Gallagher, S. Jennings, C. J. McAdam, R. B. T. Connelly, A. R. Manning, B. H. Robinson, J. Simpson, *Organometallics* **2005**, *24*, 2051–2060; e) M. Zora, C. Acikgoz, T. A. Tumay, M. Odabasoglu, O. Buyukgungor, *Acta Crystallogr., Sect. C: Cryst. Struct. Commun.***2006**, *62*, m327–m330.

[22] Selected data: **3b**, molecule 1: Ph···Ph&(1 – *x*, 2 – *y*, –*z*), parallel rings with centroid···centroid distance of 3.735(2) Å, ring slippage 1.53 Å, **3b**, molecule 2: Ph···Ph&(–*x*, 1 – *y*, –*z*), parallel rings with centroid···centroid distance of 3.641(2) Å, ring slippage 1.38 Å, **3e**: Ph···Ph&(–*x*, –*y*, –*z*), parallel rings with centroid···centroid distance of 3.565(2) Å, ring slippage 0.73 Å.

[23] The centroid···centroid distance in hexagonal graphite (space group $P6_3/mmm$) is ca. 3.65 Å and the ring slippage is ca. 1.42 Å. These values were calculated from the structural data published in P. Trucano, R. Chen, *Nature* **1975**, *258*, 136–137.

[24] a) C. A. Hunter, J. K. M. Sanders, *J. Am. Chem. Soc.* **1990**, *112*, 5525–5534; see also: b) C. A. Hunter, K. R. Lawson, J. Perkins, C. J. Urch, *J. Chem. Soc. Perkin Trans. 2* **2001**, 651–669.

[25] O. Exner, *Correlations in Organic Chemistry* (in Czech), SNTL Alfa Publishers, Prague, **1981**, pp. 74–79.

[26] a) G. L. K. Hoh, W. E. McEwen, J. Kleinberg, *J. Am. Chem. Soc.* **1961**, *83*, 3949–3953; b) W. F. Little, C. N. Reilley, J. D. Johnson, K. N. Lynn, A. P. Sanders, *J. Am. Chem. Soc.* **1964**, *86*, 1376–1381; c) W. F. Little, C. N. Reilley, J. D. Johnson, A. P. Sanders, *J. Am. Chem. Soc.* **1964**, *86*, 1382–1386.

[27] S. Lu, V. V. Strelets, M. F. Ryan, W. J. Pietro, A. B. P. Lever, *Inorg. Chem.* **1996**, *35*, 1013–1023 and references cited therein.

[28] a) A. G. Nagy, S. Toma, *J. Organomet. Chem.* **1985**, *282*, 267–275; b) R. Frantz, J.-O. Durand, G. F. Lanneau, *J. Organomet. Chem.* **2004**, *689*, 1867–1871.

[29] a) K. Sonogashira, Y. Tohda, N. Hagihara, *Tetrahedron Lett.* **1975**, *16*, 4467–4470; b) S. Takahashi, Y. Kuroyama, K. Sonogashira, N. Hagihara, *Synthesis* **1980**, 827–830.

[30] P. Štepnička, R. Gyepes, I. Císařová, V. Varga, M. Polášek, M. Horáček, K. Mach, *Organometallics* **1999**, *18*, 627–633.

[31] Z. Otwinowski, W. Minor, *HKL Denzo and Scalepack Program Package*, Nonius BV, Delft, The Netherlands. For a reference, see; Z. Otwinowski, W. Minor, *Methods Enzymol.* **1997**, *276*, 307–326.

[32] A. Altomare, M. C. Burla, M. Camalli, G. L. Cascarano, C. Giacovazzo, A. Guagliardi, A. G. G. Moliterni, G. Polidori, R. Spagna, *J. Appl. Crystallogr.* **1999**, *32*, 115–119.

[33] G. M. Sheldrick, *SHELXL97. Program for Crystal Structure Refinement from Diffraction Data*, University of Göttingen, Göttingen, Germany, **1997**.

[34] A. L. Spek, *Platon – a Multipurpose Crystallographic Tool*, Utrecht University, Utrecht, The Netherlands, **2007**. Available at http://www.cryst.chem.uu.nl/platon/.

[35] M. J. Frisch, G. W. Trucks, H. B. Schlegel, G. E. Scuseria, M. A. Robb, J. R. Cheeseman, J. A. Montgomery Jr, T. Vreven, K. N. Kudin, J. C. Burant, J. M. Millam, S. S. Iyengar, J. Tomasi, V. Barone, B. Mennucci, M. Cossi, G. Scalmani, N. Rega, G. A. Petersson, H. Nakatsuji, M. Hada, M. Ehara, K. Toyota, R. Fukuda, J. Hasegawa, M. Ishida, T. Nakajima, Y. Honda, O. Kitao, H. Nakai, M. Klene, X. Li, J. E. Knox, H. P. Hratchian, J. B. Cross, V. Bakken, C. Adamo, J. Jaramillo, R. Gomperts, R. E. Stratmann, O. Yazyev, A. J. Austin, R. Cammi, C. Pomelli, J. W. Ochterski, P. Y. Ayala, K. Morokuma, G. A. Voth, P. Salvador, J. J. Dannenberg, V. G. Zakrzewski, S. Dapprich, A. D. Daniels, M. C. Strain, O. Farkas, D. K. Malick, A. D. Rabuck, K. Raghavachari, J. B. Foresman, J. V. Ortiz, Q. Cui, A. G. Baboul, S. Clifford, J. Cioslowski, B. B. Stefanov, G. Liu, A. Liashenko, P. Piskorz, I. Komaromi, R. L. Martin, D. J. Fox, T. Keith, M. A. Al-Laham, C. Y. Peng, A. Nanayakkara, M. Challacombe, P. M. W. Gill, B. Johnson, W. Chen, M. W. Wong, C. Gonzalez, J. A. Pople, *Gaussian 03, Revision C.02*, Gaussian, Inc., Wallingford CT, **2004**.

[36] A. D. Becke, *Phys. Rev. A. At. Mol. Opt. Phys.* **1988**, *38*, 3098–3100.

[37] J. P. Perdew, Y. Wang, *Phys. Rev. B: Condens. Matter* **1992**, *45*, 13244–13249.

[38] M. Douglas, N. M. Kroll, *Ann. Phys. (NY)* **1974**, *82*, 89–155.

[39] E. D. Glendening, A. E. Reed, J. E. Carpenter, F. Weinhold, *NBO, Version 3.1*.

[40] G. Schaftenaar, J. H. Noordik, *J. Comput.-Aided Mol. Des.* **2000**, *14*, 123–134.

Received: February 1, 2008
Published Online: April 11, 2008

